MOLECULAR AND SUPRAMOLECULAR STRUCTURES AT THE INTERFACES

Methanol Oxidation on Aluminium-Copper-Silicon Alloys Coated with Polyprrole[1]

A. Büyüksağiş[a] and A. A. Aksüt[b]

[a] *Afyon Kocatepe University Faculty of Science and Art, Afyonkarahisar/TURKEY*
[b] *Ankara University Faculty of Science Chemistry Department Ankara/Turkey*
e-mail: absagis@aku.edu.tr

Abstract—Methanol oxidation on the aluminum-copper-silicon alloys which are coated with polyprrole were investigated in 1 N H_2SO_4 by using electrochemical method. For this purpose, first the current density-potential curve of alloys were obtained in 1 N $H_2SO_4 + x$ M pyrrole solutions, determined passive zones are coated with polyprrole alloys in H_2SO_4 solutions. Then the current-potential curves were obtained in 1 N $H_2SO_4 + x$ M methanol with aluminum alloys and these are expected at +1.5 V against to the standard calomel electrode (SCE) at the different times in 1 N $H_2SO_4 + 10^{-3}$ M pyrrole that were obtained with different scan rates. The extreme methanol oxidation was seen on the E110 and E140 alloys which are coated with polyprrole. Embedded pH electrode solutions which were coated with polypyrrole in 1 N H_2SO_4 and 1 N $H_2SO_4 + 0.5$ M methanol solutions were measured after 30 minutes at +2.1 V.

1. INTRODUCTION

There is an increasing interest in the electro-oxidation of methanol due to the development of direct methanol fuel cells (DMFCs) as power sources for electric vehicles and electronic devices [1–6]. However, Pt electro-catalyst is poisoned by the intermediate of methanol oxidation, such as $CO_{ads.}$ Since the mid-1970s, modification of the catalyst surface has been made by putting second metal in platinum (Pt alloys) to promote methanol electro-oxidation at platinum [7–9]. The electro-catalytic activity of platinum and platinum alloy particles for methanol oxidation depends on many factors [10, 11]. Of these, the supporting materials and their porosities are indispensable for the Pt based on catalyst to produce high catalytic activity. Akundy and Iroh [12]. The electro deposition of polypyrrole was carried out at scan rates of 750 and 50 mVs⁻¹ in oxalic acid solution. There is a considerable increase in the formation of polypyrrole on the aluminum as the number cycles is increased. Antolini and Gonzalez [13] polymer-supported metal particles also present higher tolerance to poison due to the adsorption of CO species, in comparison to the serious problem of poisoning of bulk and carbon-supported metals. Holdcroft and Funt [14] observed a slow rate of permeation of dissolved oxygen through polypyrrole. It may be feasible to improve the porosity of the polymer matrix, and by this way, the rate of permeation of solution species, by chemical attachment of bulky groups (e.g., sulphonate substituent) relating

strategic points in the molecule. A method to introduce the SO_3H groups into polypyrrole (PPy) consists in the incorporation of polystyrene sulphonate (PSS) into the PPy matrix. Qi et al. [15] deposited Pt particles on a PPy/PSS composite, prepared by chemical oxidation of pyrrole in the presence of sodium polystyrenesulphonate. They found that chemically prepared PPy/PSS has quite different ion transport properties from electrochemically prepared PPy/PSS. According to the authors, the chemically prepared material presumably adopts a structure/morphology more suitable for rapid ion (proton) transport. Li and Lin [16] electrochemically deposited Pt on a PPy nanowire matrix and formed a Pt/PPy nanocomposite on a glassy carbon electrode surface. Larger surface area and higher electrocatalytic activity for oxygen reduction reaction and methanol oxidation reaction were found at the Pt/PPy nanocomposite in comparison with pure Pt modified electrode, ascribed to the high dispersion of Pt nanoclusters in the large surface area of PPy nanowires and the synergic effect of the Pt core–PPy shell. In this work, however, the electrochemical activity of Pt incorporated in nanostructured PPy was not compared with that of Pt deposited on conventional PPy. Becerik et al. [17] tested the effect of the platinum deposition potential on PPy supports on the electrooxidation of methanol. They found that the current density increases with increasing the deposition potential, and becomes stable for deposition potentials more positive than −0.46 V vs. MSE. Azar and Habibi [18]. The electrooxidation of methanol was studied on the Al/Pd/Pt, Al/Pd/Pt covered by poly(phenylenediamines) (PPDA) and Al/Pd-modi-

---

[1] The article is published in the original.

Table 1. Chemical composition [wt] of the alloys studied in the present work

Alloy	Cu	Mg	Si	Fe	Mn	Ni	Zn	Pb	Sn	Ti	Cr
E 110	3.10	0.29	5.20	0.47	0.35	0.03	0.19	0.04	0.001	0.03	0.008
E 140	0.85	0.20	12.00	0.64	0.38	0.09	0.48	0.06	0.001	0.03	0.01
E 150	2.35	0.23	12.30	0.82	0.26	0.08	0.58	0.04	0.02	0.03	0.01
E 160	3.40	0.22	8.60	0.88	0.21	0.09	0.75	0.09	0.02	0.03	0.01
E 171	0.24	0.48	10.00	0.44	0.38	0.008	0.23	0.01	0.005	0.02	0.01
E 195	0.94	1.02	18.23	0.23	0.011	0.97	0.004	—	—	0.01	0.002

fied by PPDA dispersed platinum electrodes in 0.1 M H_2SO_4 as supporting electrolyte A comparative study of permselective properties and platinum dispersion characteristic of PPDA films toward methanol has been performed. Habibi and Azar 2010 [19] a high catalytic current for methanol oxidation was found for the polymer modified electrodes when Pt nanoparticles were embedded into the polymer films. The ortho and para (partly) derivatives show a good permeability towards methanol as well as good dispersion ability towards Pt catalyst nano-particles. The aim of the present work to examine methanol oxidation on the polyprrole coated aluminium alloys in 1 N H_2SO_4 solution by obtaining current density-potential curves with different scan rates. Pt used to use as catalyst in fuel cells. However in current researches it has been found that dual alloys of it (e.g. Pt–Ru, Pt–Sn) are more effective. Because Pt is a very expensive metal, alternative metals and alloys should be examined instead of it. Therefore in this study, Al alloys were examined as the alternatives of Pt and Pt alloys.

2. EXPERIMENTAL

Al–Cu–Si alloys were used as working electrodes. The experiments were carried out in a electrochemical cell with a working electrode, a platinum electrode and a saturated calomel electrode (SCE) were used as auxiliary and reference electrodes, respectively. All potentials were referred to the saturated calomel elec-trode. The chemical compositions of the studied Al alloys are given in Table 1.

Al alloys were 3 mm in diameter and mounted in teflon. Before each experiment the electrodes were polished with 1200 grit emery paper, washed thoroughly with bidistilled water, then transferred to the cell. During each experiment, solutions were mixed with a magnetic stirrer. Solutions were prepared bidistilled water using Merck grade H_2SO_4 pyrrole and methanol. Measurement were obtained using a system consisting of a Wenking PGS 2000D potentiostat. The synthesis of PPy film and methanol oxidation on Al alloys was achieved by using cyclic voltammetry technique. The anodic polarization curves were recorded after 20 minute of immersion of working electrode in corrosive test solution, with the scan rates 1, 5, 10, 20, 50, 100, 200 mVs^{-1}.

3. RESULTS AND DISCUSSIONS

At first, aluminium alloys covering with polypyrrole were investigated by obtaining current density-potential curves in 1 N H_2SO_4 and 1 N $H_2SO_4 + x$ M pyrrole solutions (Fig. 1).

It can be seen at Fig. 1, the working electrode surface was covered with polypyrrole at +1.5 V. The transpassive potential is began at the 3.0 V potential. The current densities of E171 alloy at the different potential on the current-potential curves obtained in 1 N H_2SO_4,
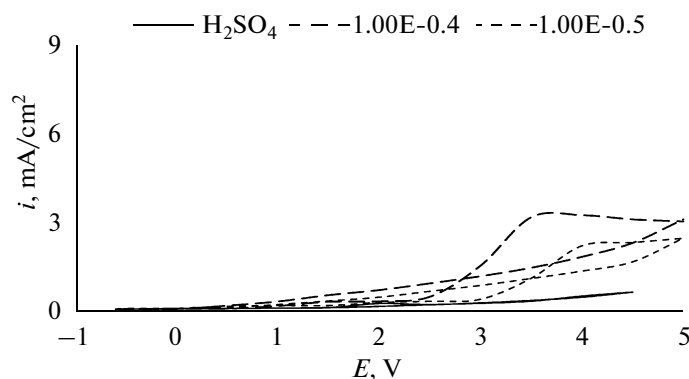

Fig. 1. The current density-potential curves of E171 alloy obtained in 1 N H_2SO_4 and 1 N $H_2SO_4 + x$ M pyrrole solutions (scan rate 20 mVs^{-1}).

Table 2. The current densities of E171 alloy at the different potentials on the current-potential curves obtained in 1 N H_2SO_4, 1 N $H_2SO_4 + x$M pyrrole solutions with scan rate 20 mV/s

	H_2SO_4	$H_2SO_4 + 10^{-4}$ M pyrrole	$H_2SO_4 + 10^{-5}$ M pyrrole
	$i\,(\mu A/cm^2)$	$i\,(\mu A/cm^2)$	$i\,(\mu A/cm^2)$
+1.5 V	67.94	127.39	127.39
+3.0 V	285.92	1132.34	1457.90

1 N $H_2SO_4 + x$ M pyrrole solutions with scan rate 20 mVs^{-1} given in Table 2.

Corrosion rates and passivity current are dependent on the waiting time at +1.5 V in 1 N $H_2SO_4 + 10^{-3}$ M pyrrole solutions. The current increases approximately at +1.5 V in containing pyrrole monomer 1 N H_2SO_4 solution. This increase was related to monomer oxidation. The oxidation current values increased again at the +3.0 V significantly. This event was explained with better monomer oxidation on freshly produced polipyrrole (PPy) film, with respect to passive Al surface [20]. The electro polymerization of pyrrole on oxidiable metals (e.g. Fe, Zn, Pb, etc.) is difficult as the metal dissolution potentials are much lower than the oxidation potential of pyrrole. The metal dissolution dominates and polymerization does not take place at all or very loosely adherent films are formed in some cases. The problem, in principle, can be solved by selecting appropriate supporting electrolyte, pretreating the metal surface, and/or varying polymerization parameters, e.g. concentration of monomer, concentration of electrolyte, pH of the electrolyte and current density. However, these changes will be associated with change in the conductivity and morphology of the film [21–22]. The current density-potential curves obtained in 1 N H_2SO_4 solution with E171 waited at +1.5 V in $H_2SO_4 + 10^{-3}$ M pyrrole solution for different times(1,5,10,20 minutes) are given in Fig. 2, with 50 and 100 mV/second scan rates respectively.

Polymerization of pyrrole was examined in E171 alloy, because this alloy shows the best passivation [23]. As it is seen in Fig. 2a, pyrrole gets polymerized about +1.5 V, transpassivity occurs about +3.5 V. As
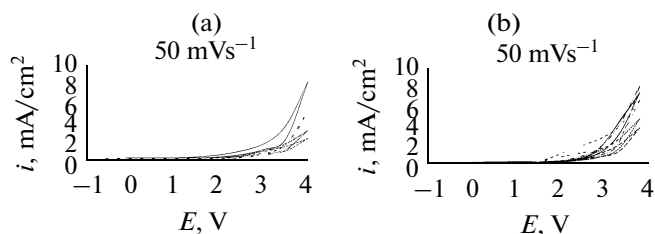
the polymer film increases, the oxygen evolution decreases. If the potential scanning rate is fast (Fig. 2b), the dissolution of passivity gets late and as a result of this the passivity region shifts to positive potential. The current densities calculated at the +1.5 V and +3.5 V in Fig. 2 are given Table 3.

Thickness of polypyrrole are dependent waiting time[24] at the +1.5 V potential in 1N $H_2SO_4 + 10^{-3}$ M pyrrole solution (Table 3). When the Table 3 is examined, with the addition of pyrrole into the solution the passivity current values decreased. This indicates that polypyrrole has a conductive structure. It is seen that Table 3 the passivity currents decrease as the waiting period of pyrrole gets longer because a thicker barrier film occurred on the alloy surface. In addition, corrosion rates were determined from extrapolation of the Tafel zones of the current density-potential curves of the alloys E140, E195 and E171 that they were obtained in 1N H_2SO_4 after different times waited in 1N H_2SO_4 or 1N $H_2SO_4 + 10^{-3}$ M pyrrole solutions. Corrosion rates were given in the Table 4.

In order to examine methanol oxidation on the aluminium alloys, electrodes were covered first by polypyrrole waited 20 minutes at +1.5 V in 1 N $H_2SO_4 + 10^{-3}$ M pyrrole then the current density-potential curves were obtained in 1N $H_2SO_4 + 10$ M methanol solution with different scanning rates (Fig. 3).

Then, the current densities-potential curves on E150 and E110 alloys were obtained in 1 N $H_2SO_4 + x$ M methanol solutions with different scan rate for understanding the effect of methanol concentration on the methanol oxidation mechanism (Figs. 4, 5).

Methanol oxidation has been observed by obtaining current potential curves between +1.5 V and +3.5 V with scanning rates 100, 50, 10, 5 mVs^{-1} in the consisting of 1 N $H_2SO_4 + x$ M methanol mediums (Figs. 3d, 3e, 3f, 4). It is observed especially in the scanning rate of 5 and 1 mVs^{-1} that while the increasing methanol concentration diminishes the oxidation peak, the decreasing of potential scanning rate enlarges the oxidation peak as it is seen on these curves (Fig. 6). Two oxidation peaks have been observed in E110 and E140 alloys coated polyprrole.

The difference among peaks potentials decreased by means of increase of methanol concentration. It is also observed that the increasing of methanol concentration as a result of decreasing potential scan rate causes the enlargement of oxidation peaks in contrast to fast potential scanning rate. This case was clearly observed in the current-potential curves obtained in the potential between +1.5 V and +3.0 V (Fig. 7). Methanol oxidation was not observed in 1 N NaCl and 1 N NaOH medium. It is resulted from pitting corrosion in Cl$^-$ medium, oxide were not seen on the surface in OH$^-$ medium because of fast dissolution. The polymer on the surface accelerates methanol oxidation (the current increases in the scanning rate 10 mVs^{-1} in E171 alloy).

Fig. 2. The current density-potential curves obtained on E171 in H_2SO_4 solution that it was waited at different times in $H_2SO_4 + 10^{-3}$ M pyrrole medium (—H_2SO_4, _ _ _ 1 min, — — — 5 min, —..—..—.. 10 min, ... 20 min).

Table 3. The passivity current densities obtained in Figs. 2 and 3 at the +1.5 V and +3.5 V

E, V	Scan rate, mVs^{-1}		Waited in $H_2SO_4 + 10^{-3}$ M pyrrole			
			1 min.	5 min.	10 min.	20 min.
		i, µA/cm^2	i, µA/cm^2	i, µA/cm^2	i, µA/cm^2	i, µA/cm^2
+1.5 V	50	212.31	99.08	84.93	84.92	59.45
	100	184.1	127.39	84.92	84.92	134.46
+3.5 V	50	3538.57	1316.35	1670.21	1571.12	1556.97
	100	2760.09	1273.89	1670.205	2547.77	2476.99

Table 4. Corrosion rates in 1 N H_2SO_4 and 1 N $H_2SO_4 + 10^{-3}$ M pyrrole solution for E140, E195 and E171 alloys with scanning rate 2 mV/s were measured

	E140 alloy		E195 alloy		E171 alloy	
	i, µA cm^2					
	H_2SO_4	$H_2SO_4 + 10^{-3}$ M pyrrole	H_2SO_4	$H_2SO_4 + 10^{-3}$ M pyrrole	H_2SO_4	$H_2SO_4 + 10^{-3}$ M pyrrole
20 min	1.70	1.72	1.60	1.62	0.70	1.18
10 min	1.56	1.57	2.23	1.50	1.32	1.00
5 min	1.60	1.66	1.60	1.17	1.47	0.70
1 min	1.55	1.66	1.57	1.58	1.70	0.50

The of passivity currents observed at +2.0 V in the current density- potential curves were obtained with scan rate 50 mVs^{-1} after waited for 1, 5, 10, 20 min in 1 N H_2SO_4 and 1 N $H_2SO_4 + 10^{-3}$ M pyrrole were found as follows.

The surface covered more when the time gets longer. It can be said that the polymer occurred on the metal surface is conductive. Methanol oxidation occurs more with decreasing scanning rates on the 110 and 140 alloys coated polypyrrole. It dissolves more in
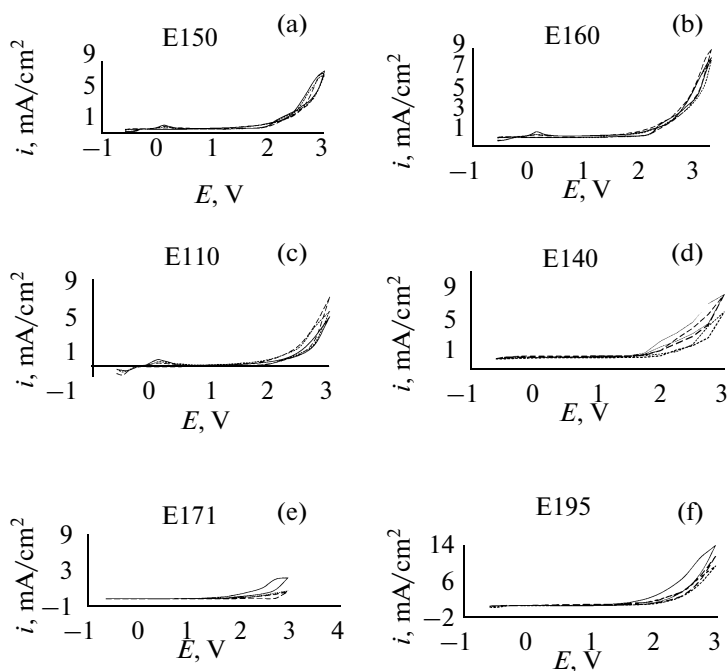
Fig. 3. Current density-potential curves for polypyrrole coated aluminum alloy in 1 N H_2SO_4 + 0.1 M methanol solution with different scan rates (—50, ... 100, - - - 200).
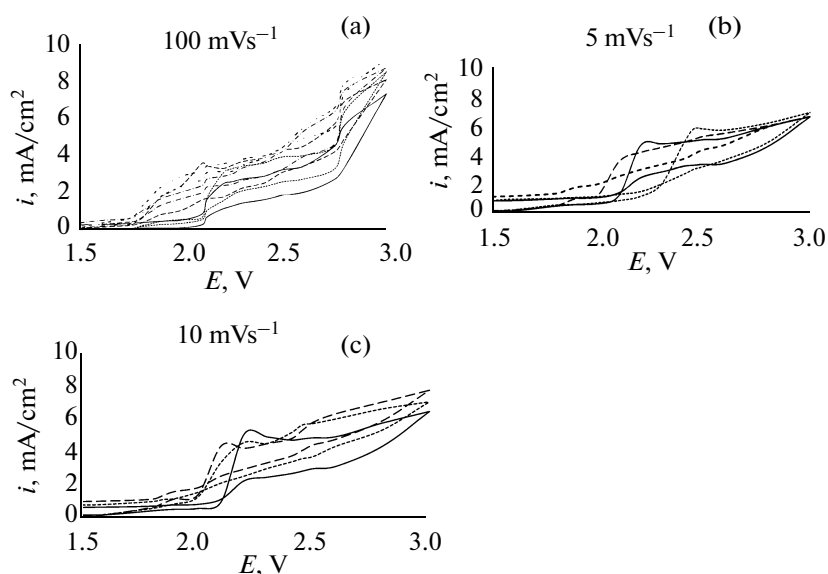
Fig. 4. Current density-potential curves for E150 alloy covered polypyrrole in 1 N H_2SO_4 + x M methanol with different scanning rate (—0.01 M, - - - 0.05 M, − − − 0.1 M, -.-.-.- 1 M, ... 3 M).
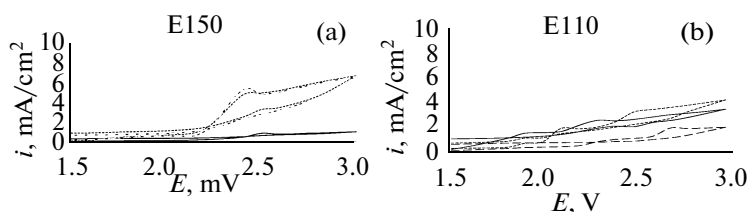

Fig. 5. Current density-potential curves obtained for aluminum alloy coated polyprrole in 1 N H_2SO_4 + 0.01 M methanol solution with different scan rate (—1 mVs^{-1}, − − − 5 mVs^{-1}, ... 10 mVs^{-1}).

1 N H_2SO_4 containing lower methanol concentration medium. Methanol oxidation occurs again prominently on the good polypyrrole film. For this result, metal surface is porous or open, oxidation occurs in a great scale. If the scanning rate is lower because of performing methanol oxidation slow and oxidation
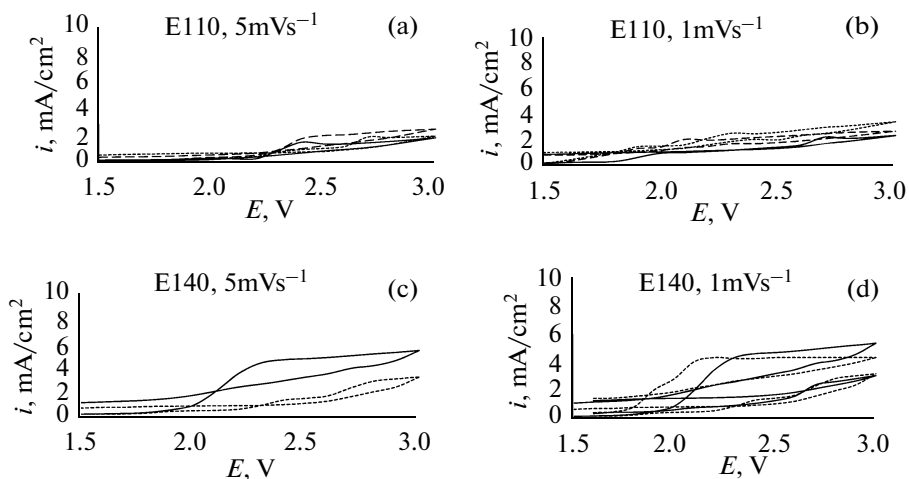

Fig. 6. Current density-potential curves for aluminum alloy coated polyprrole with different scanning rate for different methanol concentration (—0.01 M, ... 0.05 M, − − − 0.1 M).
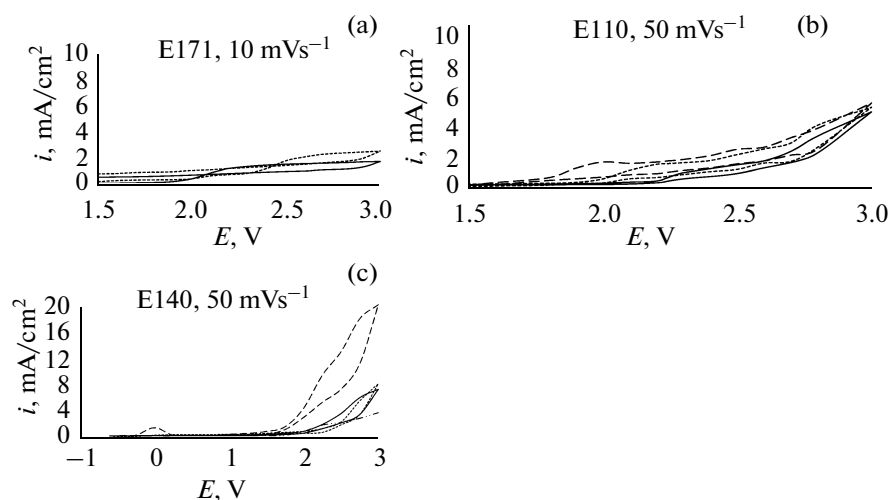
Fig. 7. Current density-potential curves for aluminum alloys coated polypyrrole with different methanol concentration (—0.01 M, ... 0.05 M, − − − 0.1 M, −..−.. 1 M).

occurs enough. It was seen from pH values before experiments and after waiting 30 minutes at +2.1 V and +2.5 V in 1 N H_2SO_4 + 0.05 M methanol solution that formic acid and CO was occurred. pH values are given in Table 6.

Small organic molecules occur during methanol oxidation. In addition, CO_2 is the major product during the oxidation methanol to the formic acid (methyl formate) and formaldehyde. Their yields depending on experimental conditions such as surface roughness and methanol concentration and time of electrolysis. Electrochemical measurements showed that CO_2 and HCOOH are also dependent on the methanol concentration and scanning rates [24−29]. The oxidation of CO_2 on the alloys occur at higher potential (approximately 2.5 V). The electro-oxidation of methanol is

not so fast and its chemisorption is not the rate-determining step, because the adsorption/dehydrogenation of methanol becomes more difficult due to alloys. The passivity currents decrease as the waiting period of pyrrole gets longer because a thicker barrier film occurred on the alloy surface. The current values waited in 1 N H_2SO_4 + 0.05 M methanol solution after different waiting times and potentials were given Table 7.

The current values increase as the waiting period of electrode (at 2.5 V) gets longer because methanol oxidation occurs on the alloy surface. In other word the current values decrease as the waiting period of electrode (at 2.1 V) gets longer form compact film occur on the alloy surface.

Table 5. Current density values at the constant potential (+2 V) obtained in 1 N H_2SO_4 waited different times in 1 N H_2SO_4 or 1 N H_2SO_4 + 10^{-3} M pyrrole solutions for E171 alloy

Time (minutes)	1 N H_2SO_4 i (mA/cm^2)	1 N H_2SO_4 + 10^{-3} M pyrrole i (mA/cm^2)
1	20	20
5	7	20
10	5	10
20	3	4

Table 6. pH values in 1 N H_2SO_4 + 10^{-3} M pyrrole + 0.05 M methanol solution

	Before experiments pH	pH value after waited 30 min at +2.1 V	pH value after waited 30 min at +2.5 V
E110	3.32	3.23	3.09
E140	3.32	3.07	3.13

Table 7. The current values waited in 1 N H_2SO_4 + 0.05 M methanol solution after different times and potentials

	+ 2.5 V (E140)	+ 2.1 V (E140)	+ 2.1 V (E110)
t (minutes)	I (μA)		
0	157	136	196
5	179	126	194
10	191	120	191
15	202	116	185
20	207	113	173
25	211	108	165
30	215	107	166

CONCLUSIONS

The electrodes were successfully used for the oxidation of methanol in acidic methanol electrolytes and preliminary results suggest that the catalyzed Al alloys is a promising alternative candidate to PtRu anode catalysts for methanol oxidation. Application and optimization of these alloys for fuel cell electrocatalysis will therefore be focus of our interest in subsequent investigations.

ACKNOWLEDGMENTS

REFERENCES

1. Habibi, B., Pournaghi-Azar, M.H., Abdolmohammad-Zadeh, H., and Razmi, H., *International Journal of Hydrogen Energy*, 2009, vol. 34, p. 2880.

2. Fuel Cell Handbook, *EG and G Services, Inc. and Science Applications International Corporation*, Morgantown, WV: US Department of Energy, 2000, 5th ed.

3. Iwasita, T., *Electrochim. Acta,* 2002, vol. 47, p. 3663.

4. Shimazu, K., Uosaki, K., Kita, H., and Nodasaka, Y., *J. Electroanal. Chem.*, 1988, vol. 256, p. 481.

5. Watanabe, M., Saegusa, S., and Stonehart, P., *J. Electroanal. Chem.*, 1989, vol. 271, p. 213.

6. Shimazu, K., Inada, R., and Kita, H., *J. Electroanal. Chem.*, 1990, vol. 284, p. 523.

7. Watanabe, M. and Motoo, S., *J. Electroanal. Chem.,* 1975, vol. 60, p. 259.

8. Götz, M. and Wendt, H., *Electrochim. Acta,* 1998, vol. 43, p. 3637.

9. Morimoto, Y. and Yeager, E.B., *J. Electroanal. Chem.*, 1998, vol. 444, p. 95.

10. Kabbabi, A., Gloaguen, F., Andolfatto, F., and Durand, R., *J. Electroanal. Chem.*, 1994, vol. 373, p. 251.

11. Coker, E.N., Steen, W.A., Miller, J.T., et al., *J. Mater. Chem.*, 2007, vol. 17, p. 3330.

12. Akundy, G.S. and Iroh J.O., *Polymer*, 2001, vol. 42, p. 9665.

13. Antolini, E. and Gonzalez, E.R., *Appl. Catalysis A: General*, 2009, vol. 365, p. 1.

14. Holdcroft, S. and Funt, B.L., *J. Electroanal. Chem.,* 1988, vol. 240, p. 89.

15. Qi, Z., Lefebvre, M.C., and Pickup, P.G., *J. Electroanal. Chem.*, 1998, vol. 459, p. 9.

16. Li, J. and Lin, X., *J. Electrochem. Soc.*, 2007, vol. 154, p. B1074.

17. Becerik, I., Suzer, S., and Kadirgan, F., *J. Electroanal. Chem.,* 2001, vol. 502, p. 118.

18. Pournaghi-Azar, M.H. and Habibi, B., *J. Electroanal. Chem.,* 2007, vol. 601, p. 5362.

19. Habibi, B. and Pournaghi-Azar, M.H., *International of Journal of Hydrogen Energy*, 2010, vol. 35, p. 1.

20. Özyılmaz, A.T., Kardaş, G., Erbil, M., and Yazıcı, B., *Appl. Surf. Sci.*, 2005, vol. 242, p. 97.

21. Rahman, S.U. and Ba-Shammakh, M.S., *Synthetic Metals*, 2004, vol. 140, p. 207.

22. Can, M., Özaslan, H., Işildak, Ö., et al., *Polymer*, 2004, vol. 45, p. 7011.

23. Buyuksagis, A., *Protection of Metals and Physical Chemistry of Surfaces*, 2010, vol. 46, no. 2, p. 134.

24. Iwasita, T., *Advances in Electrochemical Science and Engineering*, Gerischer, H. and Tobias, C., Eds., Wiley: Verlag Chemie, 1990, vol. 1, p. 127.

25. Wasmus, S. and Kuver, A., *J. Electroanal. Chem.*, 1999, vol. 461, p. 14.

26. Hamnett, A., *Interfacial Electrochemistry. Theory, Experimental and Applications*, Wieckowski, A., Ed., N.Y.: Marcel Dekker, 1999, p. 843.

27. Kabbabi, A., Faure, R., Durand, R., et al., *J. Electroanal. Chem.*, 1998, vol. 444, p. 5328.

28. Scott, K. and Argyropoulos, P., *J. Power Sources*, 2004, vol. 137, p. 228.

29. Vidakovic, T., Christov, M., and Sundmacher, K., *Electrochim. Acta*, 2004, vol. 49, p. 2179.